Railway Sciences

Study on the influence factors of HST running in the tunnels at 400 km/h

Lei Liu and Gengjie Sun
Railway Science and Technology Research and Development Center, China Academy of Railway Sciences Corporation Limited, Beijing, China
Ziwei Zhang
Key Laboratory of Urban Underground Engineering of the Ministry of Education, Beijing Jiaotong University, Beijing, China and Beijing's Key Laboratory of Structural Wind Engineering and Urban Wind Environment, Beijing Jiaotong University, Beijing, China, and
Jiaqiang Han
School of Engineering, University of Warwick, Coventry, UK

213

Received 20 December 2024
Revised 18 January 2025
Accepted 6 February 2025

Abstract

Purpose – The paper aims to clarify the operation rationality of high speed trains (HSTs) under tunnel condition with the speed of 400 km/h through representative aerodynamic factors including running drag, eardrum comfort, carriages noise, aerodynamic loads on tunnel ancillary facilities and HST, micro-pressure waves, and then put forward engineering suggestions for higher speed tunnel operation based on the analysis.

Design/methodology/approach – Based on the field measurement data of CR400AF-C and CR400BF-J tunnel operation, correlations between each aerodynamic indicators with HST speed were established. By analyzing the safety reserve of aerodynamic indicators at 350 km/h and the sensitivity of each indicator to HST speed increasing and the indicators' formation mechanism, the coupling relationship between various indicators was obtained.

Findings – The sensitivity of different aerodynamic indicators to speed variation differed. The aerodynamic indicators representing flow field around HST showed a linear relationship with HST speed including noise, eardrum comfort, aerodynamic load on HST body. The positive aerodynamic load on tunnel auxiliary facilities and the micro-pressure wave at the entrance of the tunnel have the same sensitivity to the 3th-power relation of HST speed. The over-limit proportion of micro-pressure wave was the highest among the indicators, and aerodynamic buffering measures were recommended for optimization. The open tunnel pressure relief structure is recommended, while allowing trains to pass through the tunnel at an unconditional speed of 380 km/h.

Originality/value – Comprehensive evaluation of multiple aerodynamic indicators for HST tunnel operation with higher speeds was realized. The main engineering requirements to release aerodynamic effect were identified and the optimization scheme is proposed.

Keywords 400 km/h high-speed railway operating condition, Train-tunnel aerodynamic effects, Coupling analysis, Engineering optimization

Paper type Research paper

1. Introduction

During the process of high-speed trains (HSTs) entering the tunnel, the abrupt change in blockage ratio causes strong turbulence effects, leading to aerodynamic piston effects to the

The author(s) disclosed the receipt of the following financial support for the research, authorship and/or publication of this article.

Declaration of conflicting interests: The author(s) declare no potential conflicts of interest with respect to the research, authorship, and/or publication of this article.

Railway Sciences
Vol. 4 No. 2, 2025
pp. 213-230
Emerald Publishing Limited
e-ISSN: 2755-0915
p-ISSN: 2755-0907
DOI 10.1108/RS-12-2024-0052

train-tunnel flow field. These effects have an adverse impact on the safety of tunnel structures and ancillary facilities, the operation stability of HST, passengers' eardrum comfort and surrounding environment (Wang *et al.*, 2019). During the process, compression and expansion waves are formed at the front and rear of HST, respectively, while abnormal pressure regions also develop near the nose of the front and rear carriages. The propagation and reflection of pressure waves along the tunnel, as well as their interaction with the surrounding areas of HST, will lead to flow field anomalies around HST and cause relevant train-tunnel flow field indicators to exceed the limit, which cause problems of safety, energy saving and comfort during the operation.

The adverse effects of train-tunnel aerodynamic effect drew global attention during the early operation of Japanese Shinkansen in the 20th century (Ozawa, Maeda, Matsumura, & Uchida, 1993; Maeda 1996). Since then, Japan and European countries conducted research studies on the train-tunnel aerodynamic effects for high-speed railway. Since the end of 20th century, scholars have carried out extensive research studies on various indicators of aerodynamic effects. Yamamoto provided a fluid analysis formula for the micro-pressure waves at tunnel portals, clarifying that the peak pressure value of tunnel micro-pressure wave is proportional to the pressure gradient of the tunnel compressive waves. Relevant measurement results from the Japanese Shinkansen showed that a ballasted track bed can mitigate the wave energy using the porous effect of the track ballast, and the amplitude of the micro-pressure wave is significantly lower than that of a slab track bed tunnel under the same blockage ratios and HST speed (Wang *et al.*, 2019; Maeda, 1996). Wang (2016) discussed the formation mechanism of the compression wave, clarifying that compression waves evolve during their propagation process. Stefan Adami conducted on-site measurements of pressure conditions when an HST enters the tunnel with the speed of 330 km/h, monitoring pressure at different mileages along a 1,460 m section of a double-line slab track tunnel with a cross-sectional area of 92 m^2, where they observed that the pressure gradient of compressive wave intensified as the wave propagated, increasing by a factor of 10 (Stefan, 2008). At the same time, regarding the issue of micro-pressure waves, scholars have designed various buffering measures such as tunnel portal buffering structures (Zhang, Wang, Ma, Hu, & Wu, 2016; Wang, Chang, *et al.*, 2018), shafts (Liu, 2010) and cross passages (Wang, Ren, *et al.*, 2018). However, with the further increase in train speeds, more optimizations are required to meet the limit values of micro-pressure wave (Sun, Wang, Gu, Zhang, & Ma, 2023).

The pressure fluctuations in high-speed railway tunnels also exert aerodynamic loads on the tunnel lining structure and ancillary facilities. In the case of the Sanyo Shinkansen and the Bohan High-Speed Rail tunnels in Japan, two incidents of concrete spalling in the secondary lining occurred, and investigations revealed that was due to the long-term aerodynamic load causing fatigue damage to the main concrete lining structure (Li, 2022). At the same time, ancillary structures such as lighting and ventilation in high-speed railway tunnels are at risk of failure or even intrusion into the tracks due to the long-term effects of aerodynamic loads. Moreover, HSTs under high speed face higher operation drag, which consists mainly of wheel-rail frictional drag and aerodynamic drag, which are respectively proportional to the first and second power of speed (Xiong & Deng, 2021; Deng, Liu, Li, & Zhang, 2022; Deng, Zhang, Wang, & Zhang, 2019). The drag of wheel-rail effect could be eliminated by Maglev form, while the aerodynamic drag is hard to be released under traditional HSTs' operation condition. It is worth noting that, under the operating condition of 400 km/h, the aerodynamic drag accounts for 80% of the total drag, and when the speed increases to 500 km/h, this proportion will rise to 90% (Shen, 2005). To reasonably analyze the aerodynamic drag, Raghu categorized the aerodynamic drag of HST running under open line into head-tail pressure differential drag and turbulence drag along HST body (Raghu, 2002). According to this scheme, the aerodynamic drag coefficient can be divided into pressure difference inlet drag coefficient and turbulence drag coefficient under tunnel conditions (Wang, Zhang, & Yuan, 2022). Although optimizing the train geometry and increasing the tunnel cross-sectional area could theoretically reduce aerodynamic aerodynamic drag, its feasibility is less than satisfactory due to engineering constraints.

During HST entering the tunnel, under the pressure and tensile action of air pressure, the failure of the train body, equipment compartment or undercarriage skirt occasionally occurs, with a relatively high frequency under tunnel condition mainly for the fatigue load of the train body and equipment compartment induced by aerodynamic load (Mei, Li, & Guo, 2019). There is a linear relationship between the mean value of the aerodynamic load amplitude on the HST surface and the power of 1.1∼1.3 of the blockage ratio. When trains intersect in the tunnel, the aerodynamic load is proportional to the blocking ratio to the power of 1.0–1.4 (Han, Yao, Chen, & Liang, 2017). With the running speed increases, it is necessary to adopt higher strength of the HST body to resist the aerodynamic load (Sun *et al.*, 2024).

According to the theory of action regulations of HST interior and exterior field, the internal-external pressure difference is the main cause of the transient pressure increase inside the cabin, leading to the "ear pressed" phenomenon (Wang *et al.*, 2019). Han conducted research on the pressure comfort in high-speed railway tunnels in mountainous areas and clarified the alleviating effect of improving the train body sealing performance on transient pressure. They found that the increase in sealing indicator gradually weakens the efficiency of transient pressure reduction (Han & Wang, 2009). In addition, the train's geometric structure, such as the pantograph network, car gap and the aerodynamic noise generated by the bogie, as well as the noise from wheel-rail friction vibrations, also degrade the comfort of passengers. These issues can be mitigated by optimizing the train's sealing and enhancing sound insulation performance. Mao, Zheng, and Hao (2015) proposed the Statistical Acoustic Energy Flow (SAEF) method, coupling excitations from different physical fields and loading them onto a high-speed rail SAEF model. Xiao and Kang (2009) used the Finite Element-Boundary Element (FE-BE) method to calculate the low-frequency noise inside the cabin caused by track irregularities, but did not consider acoustic excitation or interior components. Due to limitations in the degrees of freedom and computational load of the acoustic model, they were unable to solve for mid-to-high frequency noise. Sapena, Tabbal, and Jove (2012) used the Finite Element-Statistical Energy Analysis (FE-SEA) method to build a mid-frequency acoustic model of the driver's cabin, treating interior components as having an absorption coefficient. They considered the coupling of mechanical and aerodynamic noise but neglected the wheel-rail noise and the constraints between the interior components and the white body of the train.

Table 1 shows the development trends of the 6 major aerodynamic indicators mentioned above, along with the provisions in the relevant standards. The regulations with HST speed are basically derived from HST operation under lower speed and other HST forms. At higher speeds, the law between the above aerodynamic indicators and the train speed may change to a certain extent due to the variation of the inertial action and friction action of fluctuations. Meanwhile, in these standards, there are no specific limits for train operating drag and aerodynamic loads on the train body and only recommended values are provided for the aerodynamic loads on tunnel ancillary facilities. Aerodynamic effects caused by train-tunnel operations at higher speeds will have adverse impacts on safety, energy efficiency and comfort. Although existing research has conducted detailed analyses of the related patterns of various typical high-speed railway train-tunnel aerodynamic indicators, the combined applicability of multiple typical aerodynamic indicators under higher-speed train-tunnel operating conditions is still unclear. In addition to the influence of increased train speed, there are coupling relationships between the aerodynamic parameters, which contribute to their complex development patterns.

As the large-scale commercial operation of 350 km/h high-speed railway in China tends to mature, projects related to higher speed have been gradually carried out. At higher operating speeds, the route operation considering the aerodynamic problems of the tunnel needs to consider the relevant feasibility. On the one hand, the development and strengthening law of aerodynamic indicators at higher speeds may be different from that at 350 km/h. At the same time, the safety reserve values of aerodynamic indicators at 350 km/h are different, and the sensitivity to changes in speed is different. Therefore, for line operation at higher speeds, In

Table 1. Variation law of relevant aerodynamic indicator with speed and peak limits

Aerodynamic indicator	Operation drag of HST/kN	Eardrum comfort/(kPa/ns)	Aerodynamic load of HST/Pa	Compartment noise/dB	Tunnel appendages load/kPa	Micro-wave/Pa
Relation with HST speed v	Wheel-rail drag $\propto v$ Aerodynamic drag $\propto v^2$	–	$\propto v^2$	–	$\propto v^2$(approximately)	$\propto v^3$(approximately)
Limit	No explicit limit	Transient pressure≤800 Pa/3 s and 500 Pa/1s	No explicit limit	Midcarriage≤68 dB Carriage end≤70 dB	–	20 m to tunnel portal≤50 Pa 50 m to tunnel portal≤20 Pa
Recommended value	–	–	–	–	Positive load 5.9 kPa Negative load −8.9 kPa(Tube clearance area 100 m^2; HSTs meet in tunnels with 350 km/h)	–

Source(s): Wang *et al.* (2019) and National Railway Administration (2015)

particular, the feasibility and safety of tunnels under operating conditions need to be analyzed systematically.

In order to accelerate the promotion of the CR450 scientific and technological innovation project, the National Railway Group of China proposed to deepen the core technology research tasks of high-speed trains with a speed of 400 km/h, and is expected to operate at a maximum speed of 400 km/h after the speed increase. In the first half of 2022, China National Railway Group organized the preliminary trial of CR450. The world's leading comprehensive detection train CR400AF-C and CR400BF-J were adopted to carry out field tests at higher speeds under tunnel conditions in the Wushan to Wanzhou section of Zhengyu high-speed railway, which basically clarified the development trend of train-tunnel aerodynamic effect at higher speeds.

Based on this, the paper referred to the measured data of high-speed railway train tunnel operating conditions as the basis, then established the relationship between each indicator and HST speed, formed the theoretical prediction formula and analyzed the development law of the aerodynamic indicators of 350~450 km/h. The mathematical analysis models were established according to the exceedant proportion and safety margin of each indicator compared with the standard limit. The relevant conclusions can provide reference for the operation of high-speed railway tunnels with higher speeds.

2. Field measurement

2.1 Summarize

In 2022, China Railway Department organized and carried out the CR450 HST development technical condition parameter test, including 18 test contents related to aerodynamic characteristics of HSTs, tunnels and surrounding environment. A total of 28 tunnel rendezvous tests were carried out, and the maximum speed of a single train was 403 km/h. The relative maximum speed of the intersection is 806 km/h, which sets the highest world record for the tunnel intersection test of HST. The test models of HSTs included CR400AF-C and CR400BF-J, as shown in Figure 1. The field monitoring of various aerodynamic indicators in the range of 350~400 km/h was carried out under tunnel operating conditions.

Related parameters are shown in Table 2.

The experimental tunnels include the Ganxigou Tunnel, Baicungou Tunnel, Bashang Tunnel, Chaoyang Tunnel and Huangshi Tunnel. The cross-sectional shapes of these five tunnels are identical (100 m^2), and there are no aerodynamic buffering measures in place for any of the tunnels. The experimental conditions involve trains passing through the tunnels at various speeds as well as situations of constant-speed meeting. During the experiments,

CR400AF-C
(a)

CR400BF-J
(b)

Source(s): Authors' own work

Figure 1. Test train

Table 2. Variation law of relevant aerodynamic indicator with speed and peak limits

Type	Design speed/ (km/h)	Spacing/ m	Axle load/t	Length/ m	Width/ mm	Streamline length/m	Height/ mm	Static tightness/s
CR400AF-C	350	17.8	≤17	211.3	3,360	12	4,050	60
CR400BF-J	350	17.8	≤17	211.3	3,360	12.5	4,050	60

Source(s): Authors' own work

pressure load on the typical locations of the train body surface is measured using onboard pressure sensors. The calculated aerodynamic parameters for the different operational conditions of the train are derived by assigning weights to the measurement points based on the results of aerodynamic numerical simulations and model tests.

Additionally, measurement points are arranged on the ground inside the tunnel and near the tunnel portals to test the aerodynamic forces and vibration characteristics of auxiliary facilities, the distribution of aerodynamic forces on the tunnel walls and the micro-pressure wave values generated at the tunnel portal when the train passes through.

2.2 Testing results

The testing results were summed up through a variety of operation conditions. The trains passed through 5 double-track tunnels with unique cross-sectional area of 100 m^2. The total lengths of the tunnels are as follows: 11.875 km (Ganxigou Tunnel), 8.247 km (Huangshi Tunnel), 5.201 km (Chaoyang Tunnel), 1.542 km (Bashang Tunnel) and 0.628 km (Baicungou Tunnel), which could effectively characterize the overall distribution of aerodynamic effects under different tunnel lengths. Relevant aerodynamic indicators are plotted as scatter plots against the train speed, tunnel length and other factors. Curve fitting is then performed on these plots. The corresponding monitoring and data processing results obtained are as in Figure 2.

From the results, the relationships of each aerodynamic indicators to HST speed could be summarized as follows:

(1) HST operation drag (y_1):

$$y_1 = 9.60281\mathrm{E}^{-4}v^2 - 0.10604v + 11.913 \tag{1}$$

(2) Transient pressure (y_2):

$$\text{① Single HST operation}(1\text{ s}): y_{21} = 0.71143v - 126.619 \tag{2}$$

$$\text{② Single HST operation}(3\text{ s}): y_{22} = 1.18286v - 280.571 \tag{3}$$

$$\text{③ HSTs' intersection}(1\text{ s}): y_{23} = 5.14857v - 1568.71 \tag{4}$$

$$\text{④ HSTs' intersection}(3\text{ s}): y_{24} = 4.65714v - 1354.76 \tag{5}$$

(3) Aerodynamic load of HST (Differential pressure load) (y_3):

$$\text{① Single HST operation}: y_{31} = 0.01933v - 3.11152 \tag{6}$$

$$\text{② HSTs' intersection}: y_{32} = 0.05195v - 12.03405 \tag{7}$$

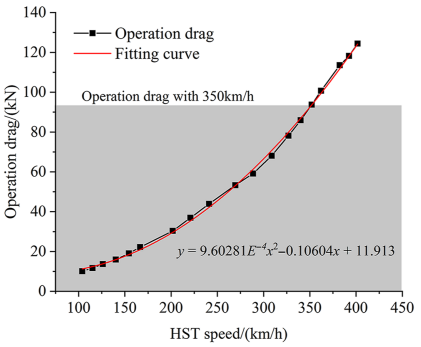

Operation drag

(a)

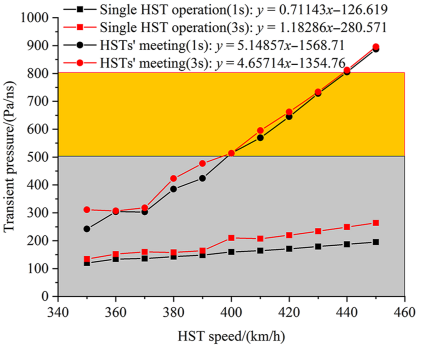

Transient pressure of compartments

(b)

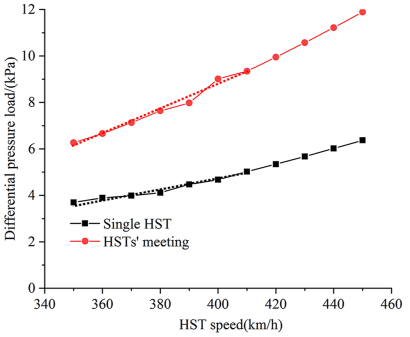

Aerodynamic load of HSTs

(c)

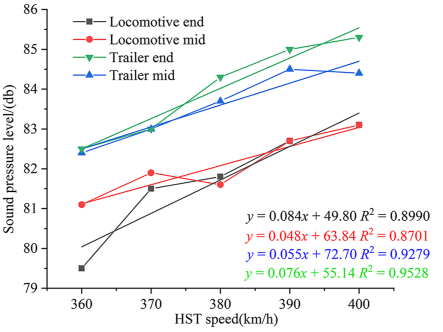

Noise in compartments

(d)

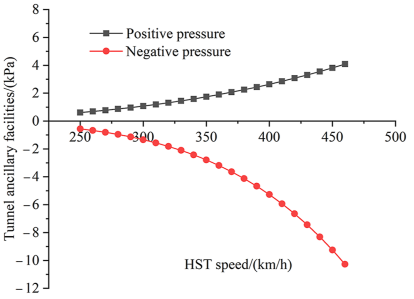

Aerodynamic loads on tunnel appendages

(e)

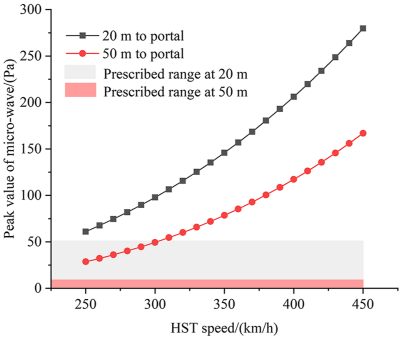

Micro-wave

(f)

Source(s): Authors' own work

Figure 2. Relative proportion and train velocity relation curve of each aerodynamic indicator

(4) Noise of compartment (y_4):

$$\text{① Mid} - \text{carriage}: y_{41} = 0.076v + 55.41 \tag{8}$$

$$\text{② Carriage end}: y_{42} = 0.055v + 72.70 \tag{9}$$

(5) Aerodynamic loads on tunnel auxiliary facilities (y_5):

$$\text{① Positive peak pressure}: y_{51} = 2 \cdot 10^{-8}\, v^{3.1208} \tag{10}$$

$$\text{② Negative peak pressure}: y_{52} = 2 \cdot 10^{-12}\, v^{4.7735} \tag{11}$$

(6) Micro-pressure waves (y_6):

$$\text{① 20 m to portal}: y_{61} = 2.91 \cdot 10^{-6}\, v^{3.124} \cdot L^{0.0468} \tag{12}$$

$$\text{② 50 m to portal}: y_{62} = 5.50 \cdot 10^{-12}\, v^{4.75} \cdot L^{0.05} \tag{13}$$

(Unit: y_1 – kN; y_2 – Pa; y_3 – kPa; y_4 – dB; y_5 – kPa; y_6 – Pa; v – km/h, L is the length of the tunnels–m)

The results showed that, the operation drag of HST basically shows the form of aerodynamic drag + wheel-rail friction drag. HST intersection will intensify the development of aerodynamic indicators. The aerodynamic load of HST resulted in the linear relationship with HST speed, as well as the compartment transient pressure and noise. The compressive aerodynamic loads on tunnel appendages represent the peak value of compressive waves, which is proportional to the 3.12 power of the HST speed, the same as the micro-pressure waves of 20 m to portal.

However, some of the indicators considered the safety evaluation in real operating condition, which resulted in some bias with former experience under ideal simulation condition or with lower HST speed.

(1) *Transient pressure in compartments:* Although the transient pressure has no clear correlation with train speed, the statistical results of a large number of measured data show that the transient pressure is proportional to HST speed.

(2) *Noise in compartments:* Under tunnel operation condition, the sound convergence and reflection effect in the narrow operating space will greatly increase the sound pressure level, but under the sound insulation effect of the car body, the growth of the noise inside the car at higher speed shows an approximate linear growth.

(3) *Aerodynamic load of HST:* The former research studies showed that the aerodynamic load around HST is proportional to the square of train speed. However, considering the damage risk mode of the HST body under aerodynamic load, it is more reasonable to adopt differential pressure load to evaluate the safety of HST body. When the pressure load inside and outside HST body changed at the same time, the pressure difference load approximately develops linearly with the speed.

(4) *Micro-pressure waves:* As for the micro-pressure wave at 50 m to tunnel portal, the peak pressure is more sensitive to the change of train speed due to the change of space elevation angle caused by side elevation slope.

Meanwhile, some indicators included the secondary indicators according to different driving schemes and measuring point positions. Considering the multiple provisions of a single aerodynamic indicator in the specification and the various running schemes of the tunnel, each seed item was discussed separately in this paper. Due to the various running cases of HST through tunnels, meanwhile in the presence of multiple secondary indicators, the requirements of indicators should be met simultaneously, and the same weight is used to select average values for different working conditions and sub-indicators during the analysis.

3. Coupling analysis

3.1 Mathematical coupling

From the perspective of mathematical coupling, the former correlation of indicators to HST speed were all of the polynomial relations. With various power exponent, the sensitivity of aerodynamic indicators to HST speed change were various. According to linear correlation theory, when two aerodynamic indicators exhibit a linear correlation, their rate of change in values is consistent with the increase in speed. Based on the fitting formula of the speed exponent, the sensitivity of 6 aerodynamic indicators to changes in speed was classified. From a mathematical perspective, this clarifies the coupling relationship between the indicators. Given the value of one indicator, the value of another aerodynamic indicator can be accurately predicted.

Based on the speed exponent, the coupling groups of the indicators are as follows:

(1) *Speed first order term:* Includes three indicators: aerodynamic load of HST, eardrum comfort and aerodynamic noise in compartments.

(2) *Speed Second Order Term + First Order Term:* HST operation drag.

(3) *Speed third order term:* Aerodynamic load positive pressure on auxiliary facilities and peak micro-pressure wave at the tunnel portal.

(4) *Speed fourth to fifth order terms:* Negative pressure aerodynamic load on auxiliary facilities.

The pattern of proportional changes with increasing speed in the above speed terms is consistent. During the testing process, the negative pressure of the aerodynamic load on auxiliary facilities took into account the effects of train speed and the relative length of the train-tunnel system. This ensured that the reflected negative pressure fluctuations, along with the negative pressure zones at the tails of the two trains, overlapped. Overall, this term is the most sensitive to changes in speed.

3.2 Mechanistic coupling

In addition to the mathematical coupling, the coupling property can also be derived from the formation mechanism of each aerodynamic indicator. From the aerodynamic indicator of first and second order terms, the interaction mechanism are as follows:

(1) From the result of mathematical coupling, the aerodynamic indicators of speed-first-order term represent the aerodynamic characteristics of the fluid field around HST. The compressive wave ahead of HST and the micro-pressure waves evolved at the tunnel entrance represent the flow field characteristics at the far point in front of HST. From the view of mechanistic analysis, the fluid area around HST acts as the form of aerodynamic loads on HST. This part of field generates aerodynamic noise under the constraint of irregular boundary around HST, and the wheel-rail friction noise is transmitted to the interior zones. Meanwhile, the differential pressure inside and around HST will cause the transient pressure around the passengers. So the coupled indicators have the progressive causal relationship.

(2) As for the third order term, as the compressive wave ahead of HST transmit to the tunnel exit, it will turn into the form of micro-waves. Then according to the positive correlation between the peak value of the micro-pressure wave and the pressure gradient of the compressive wave, the increase of HST speed in the short tunnel does not change the wave front duration, which makes the compression wave reach a higher pressure peak with the same proportional pressure gradient at the same time path under short length of tunnels.

By the coupling results of indicators, the increase of other indicators with a coupling relationship can be effectively inferred by the change ratio of a certain parameter at a higher speed.

4. Evaluation of aerodynamic indicators

According to the field measurement results above, the indicators resulted in a significant differences compared with the standard limit value. It is necessary to carry on the normalization analysis of different aerodynamic indicators, and comprehensively evaluate the overall line running quality at higher speeds according to their overrun indicators and line influence effects.

4.1 Over-limit analysis of indicators

Considering the different unit dimensions of each aerodynamic indicators, the over-limit ratio of the indicators compared with the standard value shall be evaluated by using the normalization method. In addition, according to the relevant principle of engineering design, the difference between the aerodynamic indicators and the standard value is used as a safety reserve when it is lower than the limit value. The advantage of this method is that it is simple and intuitive, and it can compress the individual data into the same range, so that it is easy to compare.

With the limit value of x_{limit} and the testing result of x_{test}, the ratio a could be estimated as Eq. (14).

$$a = (x_{\text{limit}} - x_{\text{test}}) / x_{\text{limit}} \tag{14}$$

By this way, the difference ratio of each aerodynamic indicator changes with the speed as shown as Figure 3.

The results show that all of the ratios were of negative correlation with HST speed. However, in the specification with a clear limit value of the indicators, the indicator of eardrum compartment was negative and indicated that the existing train sealing performance can meet the transient pressure requirements of 400 km/h tunnel operation.

4.2 Evaluation methods

The specific evaluation model considered the safety and rationality according to the relevant requirements of the results of each indicator, and then integrating it into the overall quality system analysis model. Although the evaluation of each aerodynamic indicator is independent, due to the complex connection network of mutual independence and mutual restriction among multiple factors, each indicator has an influence relationship with the change of speed. Considering that multi-factor decision analysis is widely used in engineering project management, it can help to evaluate the advantages and disadvantages of different options, optimize resource allocation, and carry out risk assessment and management. This method can achieve an effective balance between optimizing the operating aerodynamic indicator of high-speed railway tunnel and higher speed.

In the multi-factor decision analysis, the safety and energy saving of the reference line operation are assigned importance weight coefficients to the aerodynamic indicators. At the

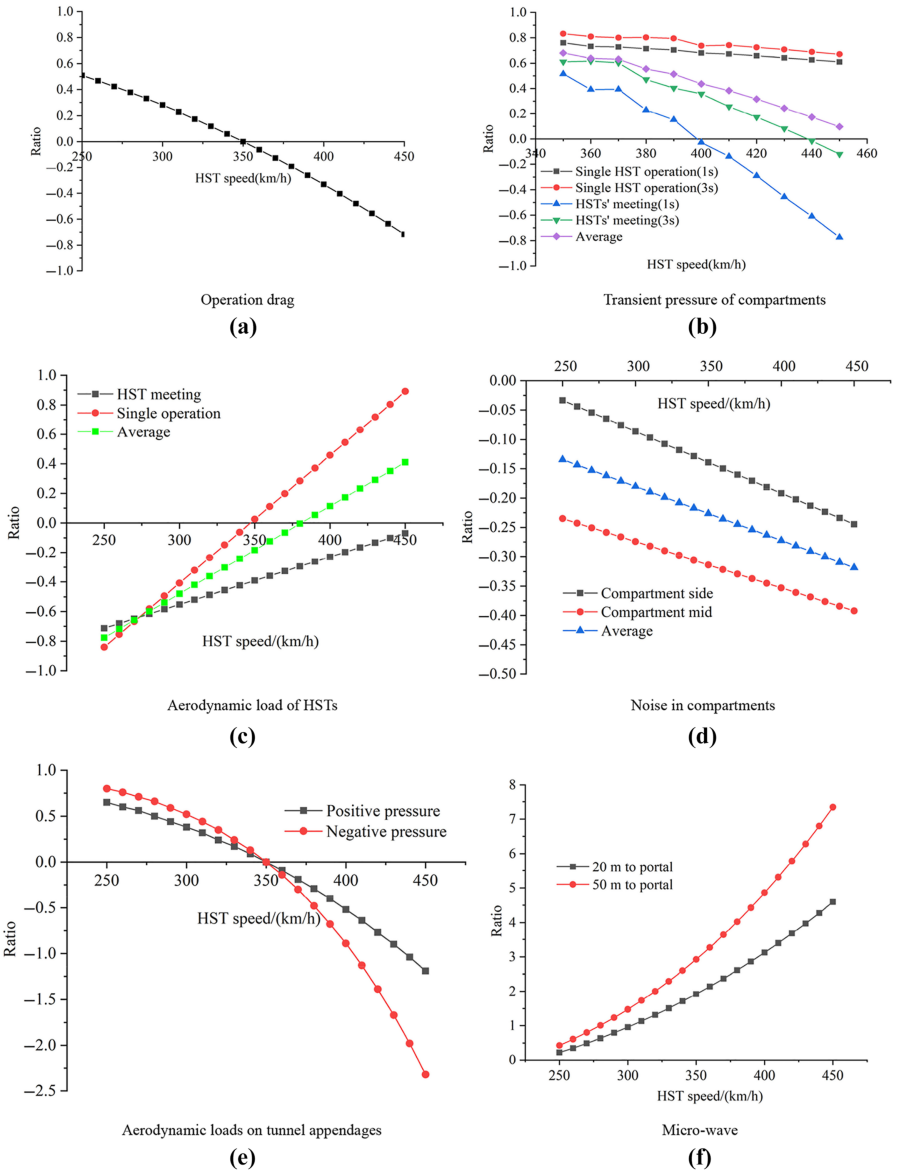

Source(s): Authors' own work

Figure 3. Relative proportion and train velocity relation curve of each aerodynamic indicator

same time, according to the coupling between aerodynamic indicators, there is a sequential causal relationship between some indicators. When reasonable engineering measures are adopted to alleviate the preceding aerodynamic indicators, the subsequent aerodynamic indicators can be further reduced. Therefore, it is necessary to assign higher weights to the preceding indicators. In addition, considering that the train running resistance at higher speeds can only be solved by using maglev in the vacuum environment of evacuated tube, which is

difficult to solve under the conditions of existing high-speed railway tunnels, and other relevant indicators can be alleviated by optimizing the train and tunnel structure. Here, the feasibility of indicator mitigation through the use of corresponding engineering measures is also included in the evaluation system of importance coefficient.

In order to avoid the bias caused by individual subjective influence in the evaluation process of each aerodynamic indicator, the influence degree of each indicator in different aspects was input into the existing artificial intelligence software Chatgpt, and the normalized weight analysis method was adopted to avoid data distortion caused by huge numerical difference between different indicators, and then artificial intelligence was used to assign weight to each indicator. The specific values are shown in Table 3.

Figure 4 helps to illustrate the evaluation method under over-limit and under-limit conditions.

(1) Figure 4(a) shows the over-limit situation of indicators. The over-limit ratio of 3 indicators are denoted as a_1, a_2 and a_3, and the importance weight coefficients are k_1, k_2 and k_3, respectively. The final overall evaluation result for the overlimit indicators could be expressed as Eq. (15):

Table 3. Importance weight coefficients of each aerodynamic indicators

	Impact in various aspects				
Indicator	Security	Energy saving	Coupling effect	Mitigation feasibility	Normalized importance coefficient k
Operation drag	Not close	Close	None	Hard	0.35
Aerodynamic load on HST	Close	Generally close	Exist	Possible	0.15
Aerodynamic load on tunnel appendages	Close	Generally close	None	Possible	0.15
Micro-wave	Generally close	Uncorrelated	None	Possible	0.20
Compartment noise	Not close	Uncorrelated	None	Possible	0.075
Eardrum comfort	Not close	Uncorrelated	None	Possible	0.075
Sum					1

Source(s): Authors' own work

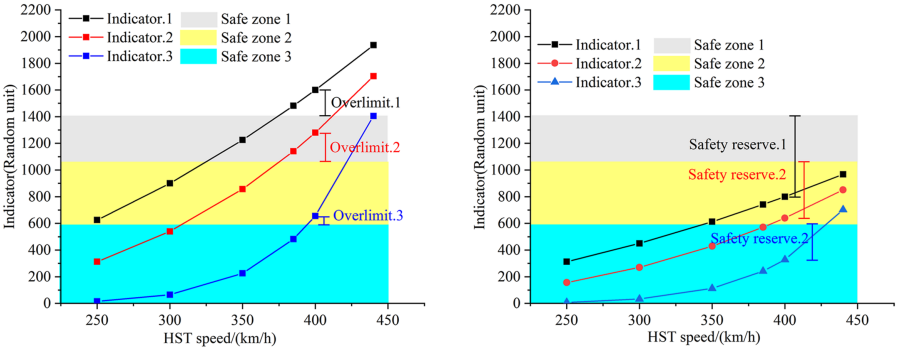

Over-limit condition (a) Under-limit condition (b)

Source(s): Authors' own work

Figure 4. Over-limit and reserve value of aerodynamic indicator

$$S_1 = k_1 a_1 + k_2 a_2 + k_3 a_3 \tag{15}$$

(2) Figure 4(b) shows the condition that the indicators are not exceeded the limitation. According to the relevant principle of engineering design, the indicator under the condition of not reaching the limit value has a certain safety reserve value, which is conducive to the improvement of the operation quality of the high-speed train tunnel. The safety reserve values of the indicators were denoted as a_4, a_5 and a_6, and the importance weight coefficients were k_4, k_5 and k_6, respectively. Finally, the overall evaluation result for the under-limit indicators is shown as Eq. (16):

$$S_2 = k_4 a_4 + k_5 a_5 + k_6 a_6 \tag{16}$$

(3) Considering the joint action of aerodynamic indicators over-limit and under-limit comprehensively, the final line operation quality evaluation indicator $S=S_2$-S_1, the higher the parameter value, the safer and more scientific the line operation.

4.3 Evaluation result

The overall score of scheme 1 and Scheme 2 and the over or under-limit ratios and the scores of indicators are shown in Figures 5 and 6, respectively.

The results revealed the over-limit and reverse ratio of indicators, HST speed sensitivity and score distribution under different importance coefficients of aerodynamic indicators. The regulations could be summarized that:

(1) The results of evaluation scheme comparing with limitation shows that the proportion of micro-pressure wave occupied a dominant position compared with other indicators. This is because there is no aerodynamic buffer measure in the test tunnel, and the efficiency of micro-pressure wave peak value and velocity growth is relatively high in the above aerodynamic indicators.

(2) The score of each aerodynamic indicator is negatively correlated with the speed, and for the aerodynamic indicator with the power indicator ≥1 of the relation with the speed, the attenuation efficiency increases at higher speeds. In the conditions of 350 to 400 km/h, compared with 300 to 350 km/h, the increase in the amount of pneumatic indicators, compared with the need for more stringent pneumatic buffer measures or

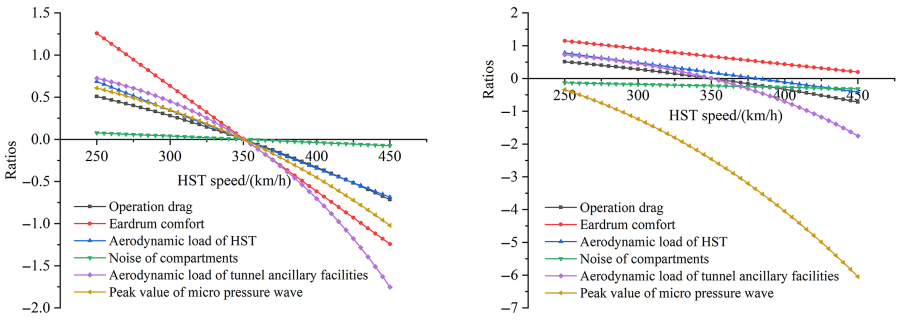

Source(s): Authors' own work

Figure 5. Over/under-limit ratios of indicators

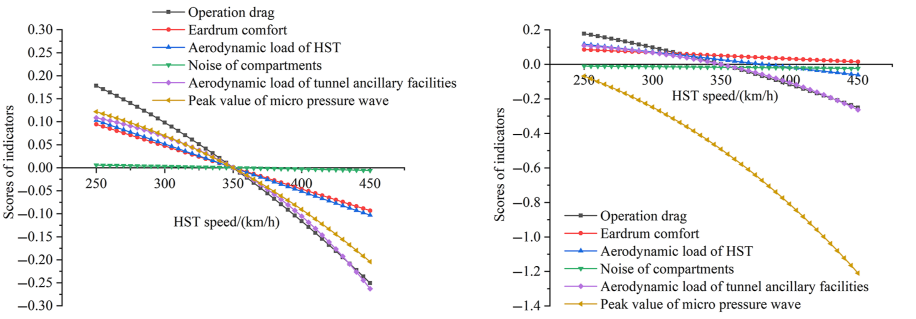

Source(s): Authors' own work

Figure 6. Scores of indicators

equipment strength improvement to ensure that the aerodynamic indicators meet the operational requirements.

(3) Under the existing train conditions, the pressure comfort indicator (transient pressure) of evaluating the train interior meets the standard requirements. This proves that cabin pressure comfort is not a controlling factor for the operation of the higher speed HST tunnel, and the train system adopted can meet the requirements of the transient pressure of the HST capsules.

4.4 Engineering recommendation for higher speed

From the evaluation results above, the engineering proposals could be put forward as followed, which rank a series of engineering proposals in order of importance and feasibility:

(1) *Recommendation 1:* Slow down the HSTs

HSTs could be slowed down during tunnel operation, which needs to determine the standard of deceleration. Since the program evaluation system in Chapter 4 is essentially determined by using the over-limit and under-limit ratios of aerodynamic indicators, for the determination of the speed reduction standard, the score over-limit situation is adopted for evaluation, and three levels are set up, respectively, with negative scores in the three stages of 0–0.25, 0.25–0.5 and 0.5–1.0, as shown in Figure 7.

In Figure 7:

(1) Zone I is of the range of negative score 0–0.25. Compared with the result of 350 km/h, the tunnel passing speed of HST could be selected below 380 km/h. Compared with the result of 350 km/h, the deterioration of the result is not obvious, and it is considered that it can be operated for a long time;

(2) Zone II is in the negative range of 0–0.25, compared with the result of 350 km/h, the aerodynamic results of 400 km/h are distributed in the acceptable range of zone II. In principle, the iterative upgrade of the HST body, tunnel facilities can greatly reduce the related safety accidents, but for the existence of certain risks, and attention and monitoring should be strengthened;

(3) Zone III is negatively divided into a range of 0.50–1.00, which is not recommended for commercial operation of the high speed railway line.

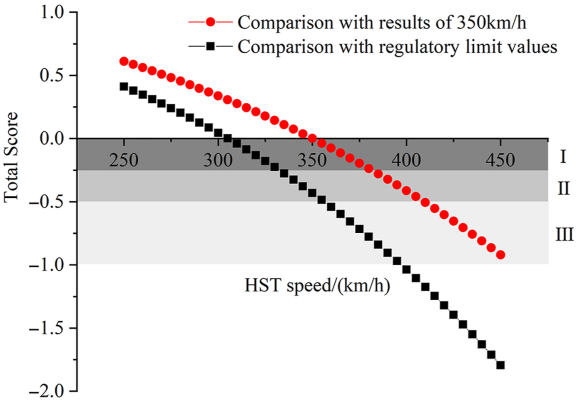

Source(s): Authors' own work

Figure 7. Selection of reasonable speed control standards

(2) *Recommendation 2:* Opening vertical shafts, inclined shafts, cross passages and pressure relief caverns for long high-speed railway tunnels (if possible)

In the early high-speed railway construction in China, the design of double hole and single track is used. Compared with the standard 100 m^2 design of the double-line tunnel, the double-hole single-line design uses two sets of 70 m^2 tunnel design. For long tunnels, it is necessary to use vertical shafts and inclined shafts to increase the construction surface during the construction phase and alleviate the aerodynamic effect during operation. For the double-line long tunnel, it is necessary to set up a cross passage to realize the evacuation of personnel during the tunnel disaster, and the aerodynamic effect could also be released by this way.

(3) *Recommendation 3:* Strengthen the aerodynamic optimization effect of the buffer structure (ensure that the basic requirements are met)

According to the variation law of each aerodynamic indicator, the exceedence ratio of micro-pressure wave is the largest compared with the standard limit values. At the same time, because the change of the peak value of micro-pressure wave with the increase of speed is more sensitive, it is recommended to lengthen the portal structure of the tunnel entrance, so as to ensure the rationality of the design of this part. Under the precondition of conditions, the micro-pressure wave peak can be reduced together with the buffer measures inside the tunnel.

(4) *Recommendation 4:* Mechanical reinforcement of train and tunnel facilities (should be further strengthened)

According to the change result of the obtained aerodynamic indicator at higher speed, the mechanical compression and suction effect will be generated on the related structure of the HST body and the tunnel auxiliary structure under higher air pressure load. In this paper, the related results are the results of the train passing through the tunnel once. Under long-term cyclic load in actual working conditions, the ability of the relevant setting to resist external load will be reduced. In particular, according to the article, the negative pressure of the tunnel auxiliary structure is the most sensitive to the change of speed increase, which should be paid special attention to.

(5) *Recommendation 5*: Enhanced sealing performance of HST (other recommendations)

In the obtained pressure comfort and noise results, only the transient pressure within 1 s inside the tunnel is above the limitation. However, in the tunnel operation condition,

because the relevant standards of noise are used in the open line operation, the internal noise under the tunnel condition is beyond the limit, and considering the relatively good air tightness, it is inferred that more noise is caused by wheel-rail vibration and friction, so it is recommended to start from the structure of the bottom of the train to enhance the sound insulation performance.

5. Conclusion

In this paper, the field measured results of CR400AF-C and CR400BF-J through the tunnel were analyzed, and the coupling relationship of aerodynamic indicators was revealed from two aspects of mathematics and mechanism by establishing the relationship between typical aerodynamic indicators and HST speed. Then, a tunnel line operation quality evaluation system model is established, and multi-factor decision analysis was adopted to clarify the development law of the overall line operation quality under different train speeds. The conclusions are as follows:

(1) Aiming at the mathematical coupling of aerodynamic indicators, by establishing the relationships expression between aerodynamic indicators and HST speed, the coupling relationships were established based on the linear correlation theorem under the same operating conditions. Among them, the two sets of parameters (1) HST aerodynamic load, eardrum comfort and the aerodynamic noise; and (2) aerodynamic load on tunnel auxiliary facilities and the positive pressure of micro-pressure wave peak value have coupling relationships, which showed linear and quadratic increasing relationship with train speed respectively. The train running drag and the negative pressure of the aerodynamic load of the tunnel auxiliary facilities are positively correlated with the square and 4–5 power of the speed respectively.

(2) According to the mechanism coupling of each aerodynamic indicator, the first power correlation to HST speed were all the indicators related to the flow field around HST, and the third direction was the indicator related to the compression wave under the train-tunnel operation. It is proved that the effect of the increase of running speed on the flow field around the vehicle in the tunnel and the space away from the HST body flow field is different.

(3) With the increase of HST running speed, the performance requirements of the facilities related to the line show a slope increase trend. This increase is not only limited by the over-limit results of the operational aerodynamic indicators, but also closely related to the final operational quality indicators. When the speed is increased from 300 to 350 km/h, the improvement in the performance of the relevant facilities is more gradual. However, when the speed is further increased to 400 km/h, the improvement in facility performance is significantly increased. In other words, a speed increase from 350 to 400 km/h requires a significantly more severe increase in facility performance than the required increase from 300 to 350 km/h.

(4) Under the operating conditions with the speed of 400 km/h, it is recommended to reduce the train speed to 380 km/h to effectively control the aerodynamic effect. During tunnel operation, it is necessary to open the pressure relief structure in the tunnel as much as possible, which has a certain releasing effect on a number of aerodynamic indicators. At the same time, the study results show that the airtight performance of the train is sufficient to meet the transient pressure requirements of higher speeds through the tunnel, and the mechanical strength of the tunnel ancillary facilities needs to be further improved.

Reference

Deng, Z., Zhang, Y., Wang, B., & Zhang, W. (2019). Present situation and prospect of evacuated tube transportation system. *Journal of Southwest Jiaotong University, 54*(05), 1063–1072. doi: 10.3969/j.issn.0258-2724.20180204.

Deng, Z., Liu, Z., Li, H., & Zhang, W. (2022). Development status and prospect of maglev train. *Journal of Southwest Jiaotong University, 57*(03), 455–474+530.

Han, H., & Wang, Y. (2009). Research of passenger eardrum comfort in long tunnel on passenger railway line in mountainous area. *Journal of Shiazhuang Raiwayinstiute (Natural Science), 22* (02), 68–72. doi: 10.13319/j.cnki.sjztddxxbzrb.2009.02.011.

Han, Y., Yao, S., Chen, D., & Liang, X. (2017). Influential factors of tunnel pressure wave on high-speed train by real vehicle test. *Journal of Central South University, 48*(5), 1404–1412. doi: 10.11817/j.issn.1672-7207.2017.05.037.

Li, F. (2022). *Research on the force characteristics of segments and bolts under the aerodynamic effect and multi-field coupling of high-speed rail shield tunnels*. Beijing Jiaotong University.

Liu, P. (2010). *Study shaft on the influence to aerodynamic effect of the high-speed railway tunnel*. Southwest Jiaotong University.

Maeda, T. (1996). Micro-pressure wave radiating from tunnel portal and pressure variation due to train passage. *Quarterly Report of RTRI, 37*(4), 199–203.

Mao, J., Zheng, X., Hao, Z., Sun, Q., & Ma, X. (2015). Calculation of full-spectrum interior noise of high-speed train with SAEF method. *Journal of Tianjin University, 48*(11), 960–968. doi: 10.11784/tdxbz201404101.

Mei, Y., Li, M., & Guo, R. (2019). Aerodynamic load distribution characteristics of pressure wave when trains passing each other in high speed railway tunnel. *China Railway Science, 40*(6), 60–67. doi: 10.3969/jissn1001-4632.2019.06.08.

National Railway Administration (2015). *TB10621-2014/J1942-2014 design specifications for high-speed railways*. Beijing: China Railway Publishing House.

Ozawa, S., Maeda, T., Matsumura, T., & Uchida, K. (1993). Micro-pressure waves radiating from exits of Shinkansen tunnels. *Railway Technical Research Institute Quarterly Reports, 34*(2), 134–140.

Raghu, S., Kim, H. D., & Setoguchi, T. (2002). Aerodynamics of high-speed railway train. *Progress in Aerospace Sciences, 38*(38), 469–514. doi: 10.1016/s0376-0421(02)00029-5.

Sapena, J., Tabbal, A., Jove, J., & Guerville, F. (2012). Interior noise prediction in high-speed rolling stock driver's cab: Focus on structure-borne paths (mechanical and aero sources). *Noise and Vibration Mitigation for Rail Transportation Systems, 118*(1), 445–452.

Shen, Z. (2005). On developing high speed evacuated tube transportation in China. *Journal of Southwest Jiaotong University,* (02), 133–137.

Stefan, A., & Hans-Jakob, K. (2008). Sensitivity of the wave-steepening in railway tunnels with respect to the friction model. *Bluff Bodies Aerodynamics and Applications Milano, Italy, July,* 20–24.

Sun, H., Wang, Y., Gu, L., Zhang, Z., & Ma, W. (2023). Study on the effect of buffer structure opening rate on micro-pressure wave at the exit and entrance of 400km/h high-speed railway tunnel. *Journal of Railway Science and Engineering, 21*(02), 433–443. doi: 10.19713/j.cnki.43-1423/u.T20230480.

Sun, G., Liu, L., Bai, X., Bai, Y., Chen, A., Gao, P., . . . Li, Y. (2024). Scientific research test on tunnel aerodynamic effects for the Guiyang-Guangzhou railway speed upgrade. *China Railway,* 10, 163–171. doi: 10.19549/j.issn.1001-683x.2024.02.27.002.

Wang, H. (2016). *Wavefront evolution during the propagation of compression wave and micro-pressure wave*. Southwest Jiaotong University.

Wang, Y., Chang, Q., Ren, W., & Zhang, L. (2018). Seam opening tunnel buffer structure aerodynamic characteristic research. *Journal of Railway Science and Engineering, 15*(01), 17–23. doi: 10.19713/j.cnki.43-1423/u.2018.01.003.

Wang, Y., Ren, W., Luo, Y., & He, J. (2018). Analysis of effect of cross adit on train-tunnel aerodynamic multiple peak characteristics. *Journal of Southwest Jiaotong University, 53*(03), 427–433. doi: 10.3969/j.issn.0258-2724.2018.03.001.

Wang, Y., Gao, B., Zhu, D., Xiao, M., Xu, X., & Zhao, W. (2019). *Aerodynamic effect control technology of high-speed railway tunnel*. China Railway Publishing House.

Wang, Y., Zhang, Z., & Yuan, J. (2022). Analysis of aerodynamic drag coefficient of the train in tunnel. *Journal of Railway Engineering Society, 39*(11), 75–80.

Xiao, Y., & Kang, Z. (2009). Acoustic contribution analysis of passenger roam of high speed train under wheel rail excitation. *Journal of South China University of Technology Normal Science Edition, 37*(2), 98–101.

Xiong, J., & Deng, Z. (2021). Research progress of high speed maglev rail transit. *Journal of Traffic and Transportation Engineering, 21*(01), 177–198. doi: 10.19818/j.cnki.1671-1637.2021.01.008.

Zhang, J., Wang, S., Ma, Z., Hu, X., & Wu, J. (2016). Research on the design method of high-speed railway tunnel buffer structure. *Journal of Railway Society, 15*(01), 17–23. doi: 10.19713/j.cnki.43-1423/u.2018.01.003.

Corresponding author
Gengjie Sun can be contacted at: 786443887@qq.com

Gengjie Sun graduated from Beijing Jiaotong University. He is an associate researcher at China Academy of Railway Sciences Corporation Limited. His research focuses on speed increase technology for high-speed railways, especially the high-speed railway capability of reaching speed of 400 km/h. In recent years, he has spearheaded multiple significant related projects and achieved fruitful results.